ISSN 0001-4370, Oceanology, 2022, Vol. 62, No. 3, pp. 289–302. © Pleiades Publishing, Inc., 2022.
Russian Text © The Author(s), 2022, published in Okeanologiya, 2022, Vol. 62, No. 3, pp. 341–356.

MARINE PHYSICS

Peculiarities of Formation of the Density Field in Mesoscale Eddies of the Lofoten Basin: Part 2

V. V. Zhmur[a, b], E. V. Novoselova[a, *], and T. V. Belonenko[a]

[a] *St. Petersburg State University, St. Petersburg, Russia*

[b] *Shirshov Institute of Oceanology, Russian Academy of Sciences, Moscow, 117218 Russia*

**e-mail: e.novoselova@spbu.ru*

Received September 27, 2021; revised December 16, 2021; accepted February 25, 2022

Abstract—This paper continues the studies of the authors of the Brunt–Väisälä (BV) frequency changes caused by mesoscale eddies of various polarities. In Part 1, we discussed the theoretical conclusions, whereas Part 2 provides the interpretation of these results on the basis of natural data. The studied region is the Lofoten Basin of the Norwegian Sea. The analysis considers the data of GLORYS12V1 oceanic reanalysis at June 10, 2010. Two eddies are considered: a quasi-permanent anticyclone, Lofoten eddy (LE), located in the center of the basin and a cyclone located southeast of LE. The mathematical formulas are verified, the characteristics of eddies are calculated, and the profiles and vertical sections of potential vorticity and BV frequency are studied. Combined analysis of natural and theoretical material results in indirect estimation of eddies, which cannot be directly measured and modeled.

Keywords: mesoscale eddies, potential vorticity, Brunt–Väisälä frequency, buoyancy frequency, Lofoten Basin

DOI: 10.1134/S0001437022030171

1. INTRODUCTION

The Lofoten Basin is a depression in the bottom topography of the Norwegian Sea with a maximum depth of 3250 m; it is limited by coordinates 5° W–20° E and 64°–76° N [1]. Being an isolated topographical unit, the basin is located between the Mohn Ridge in the northwest, the Scandinavian Peninsula in the east, and the Vorning Plateau in the south (Fig. 1). The Lofoten Basin is a dynamically active regions of the World Ocean and is characterized by higher vortex activity. The main circulation elements in the region include the branches of the Norwegian Current: slope, frontal, and coastal. The instability of these currents results in favorable conditions for the formation of mesoscale eddies [22, 23], which detach from the current flow and move under influence of topographical inclinations and β-effect, forming several main corridors of their movement [13, 17, 27].

To study the changes in the Brunt–Väisälä (BV) frequency in cyclones and anticyclones, we chose two eddies (Fig. 2a). The changes in the BV frequency was analyzed relatively so-called background BV frequency N_0 (or BV frequency in rest). The choice of an appropriate profile is not simple: Figure 2b shows that the basin is saturated by mesoscale eddies. In fact, an algorithm of automatic identification and tracking eddies applied to satellite altimetric data allowed the identification of 166000 cyclonic and 169395 anticyclonic eddies in the Lofoten Basin from 1993 to 2017. The eddies redistribute the heat and salt along the water basin [15], therefore, significantly affecting the changes in the BV frequency. Being a transitional zone for warm and saline Atlantic water masses moving to the Arctic Ocean, the Lofoten Basin plays an important role supporting the global longitudinal thermohaline circulation in the area, where Atlantic water masses radiate heat to the atmosphere, mix with ambient waters, and undergo transformation necessary for the formation of deep waters [8, 9]. The analysis of mesoscale dynamics, which was conducted by tracks of long-lived (>35 days) eddies, allowed the identification of 120 cyclonic and 210 anticyclonic eddies linked into tracks in the basin [27]. At least, two scenarios of eddy formation are found in the Lofoten Basin: (i) the detachment of meanders from a stream of the Norwegian Current or (ii) the generation of eddies at the slopes of the basin, where the velocity of the current is low [12, 17, 24].

The quasi-permanent anticyclonic Lofoten eddy (LE) is a striking feature of the basin [2, 7, 24]. Winter convection facilitates the presence of this unique natural phenomenon providing favorable conditions of its annual regeneration [11, 10]. Another scenario supporting high anticyclonic vorticity in the center of the basin is a merging with mesoscale anticyclonic eddies separated from the Norwegian Current [16]. It is known that the vicinities of large anticyclones often contain stable cyclones or ringlets [3, 5, 6, 19–21]. In fact, the LE

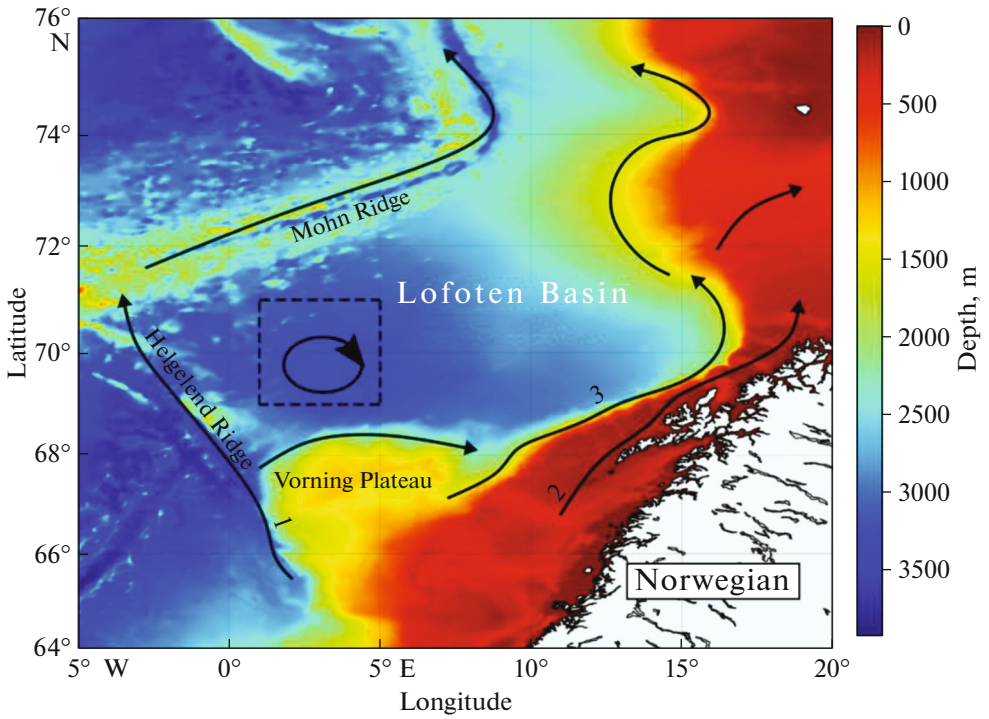

Fig. 1. Study area. The area of most possible position of the Lofoten eddy is shown by dotted line and arrow [25, 2]. The color scale reflects the character of the bottom topography. Black arrows show the branches of the Norwegian Current: (1) Frontal Current; (2) Coastal Current; (3) Slope Current.

margins also exhibit the formation of cyclones, which form a system of jointly rotating eddies together with the Lofoten Anticyclone [14].

The vertical extension or compression of elementary liquid volumes changes the BV frequencies. In this work, on the basis of empirical data, we consider the effect of mesoscale oceanic eddies on reconstruction of the BV frequency, which increases during the intensification of stratification of seawater and decreases in poorly stratified waters. The presence of eddies leads to the deformation and displacement of isopycnals, which represent the horizontal surfaces in calm ocean in the absence of eddies and the strongest deformation will be typical of those parts of isopycnic surfaces, which occur inside the eddy core or are close to it. In this article, we used the approaches published in the first part of [26]. The aim of the study to verify previous conclusions, as well as estimate changes in the BV frequency related to how mesoscale oceanic eddies affect the stratification of water.

2. MATHEMATICAL FORMULATION OF TASK: POTENTIAL VORTICITY, DENSITY FIELD, AND BRUNT–VÄISÄLÄ FREQUENCY. MAIN FORMULAS

We rely on the equity of a quasi-geostrophic approach to these events, which maintains the conservation of potential eddy for a moving liquid particle. Below, for the sake of consistent presentation of data, we provide the mathematic equations, which will be used for the estimation of various physical parameters of vortices [26].

In the coordinate system with two horizontal axes (x, y) and vertical axis z, the potential vorticity σ is expressed as the function of current $\psi(x, y, z, t)$, where t is the time and f is the Coriolis parameter [4]:

$$\sigma = \Delta_h \psi(x, y, z, t) + \frac{\partial}{\partial z} \frac{f^2}{N^2} \frac{\partial \psi(x, y, z, t)}{\partial z}. \quad (1)$$

Here, $\Delta_h \psi = \mathrm{rot}_z \vec{u}$. In a general case, the BV frequency $N(z)$ depends on the vertical coordinate z. At the constant BV frequency N_0, the equation σ is as follows:

$$\sigma = \mathrm{rot}_z \vec{u} + \frac{\partial^2 \psi(x, y, \tilde{z}, t)}{\partial \tilde{z}^2}, \quad (2)$$

where $\tilde{z} = \frac{N_0}{f} z$ is the extended vertical coordinate.

If the primary liquid at rest with constant BV frequency N_0 set in motion described by the function of the current $\psi(x, y, \tilde{z}, t)$, then the new distribution $N^2(x, y, z, t)$ will be

$$N^2(x, y, z, t) = N_0^2 \left\{ 1 + \frac{1}{f} \frac{\partial^2 \psi(x, y, \tilde{z}, t)}{\partial \tilde{z}^2} \right\}. \quad (3)$$

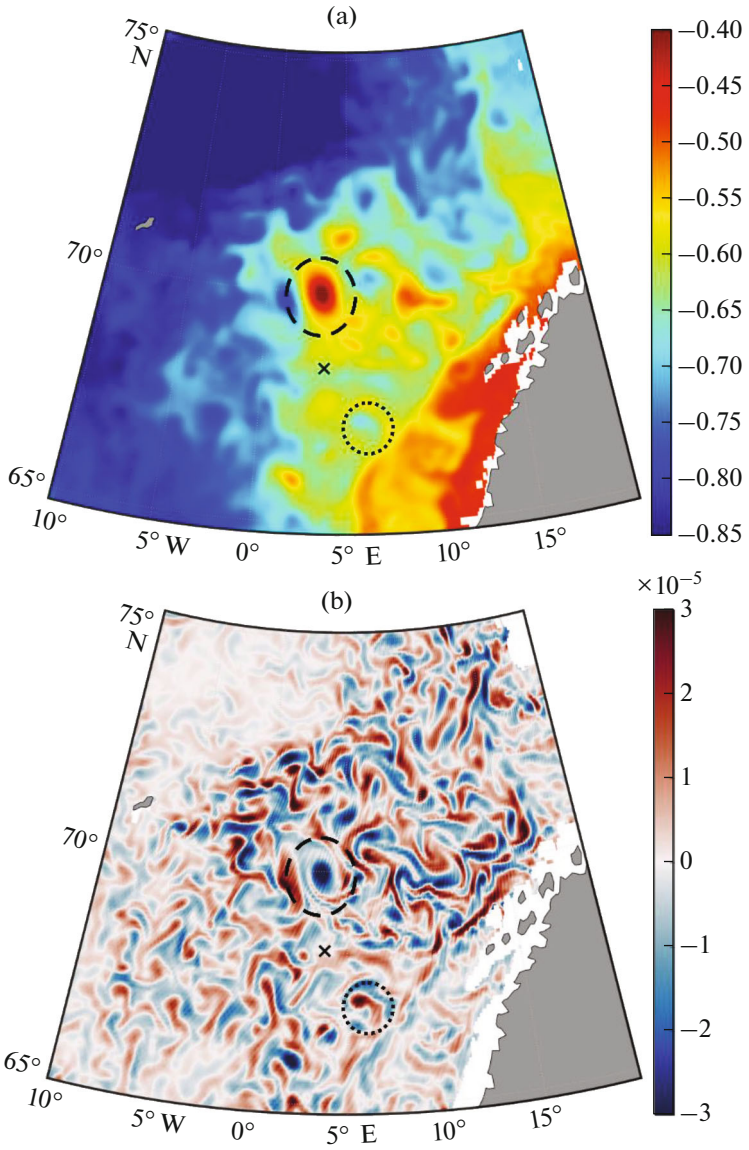

Fig. 2. Anomalies of the level, m (a) and relative vorticity at a depth of 100 m, s^{-1} (b). Black circles indicate the chosen cyclone (dots) and anticyclone (dotted line). Black cross marks the position of the point with profile of the background BV frequency.

For the ellipsoidal cores of eddies (in terminology of [26]) homogeneous by potential vorticity, we obtain

$$\mathrm{rot}_z\vec{u} = \frac{1}{2}\sigma K\int_0^\infty \frac{(2\tilde{\mu}+\nu)\,d\tilde{\mu}}{\left(K^2+\tilde{\mu}\right)^{\frac{1}{2}}\left(\tilde{\mu}^2+\nu\tilde{\mu}+1\right)^{\frac{3}{2}}}, \qquad (4)$$

$$\frac{\partial^2\psi}{\partial\tilde{z}^2} = \frac{1}{2}\sigma K\int_0^\infty \frac{d\tilde{\mu}}{\left(K^2+\tilde{\mu}\right)^{3/2}\left(\tilde{\mu}^2+\nu\tilde{\mu}+1\right)^{1/2}}, \qquad (5)$$

with the following properties of eddies, the relative vorticity $\mathrm{rot}_z\vec{u}$ and the $\frac{\partial^2\psi}{\partial\tilde{z}^2}$ value are constant inside the core (irrespectively from the point coordinates in the core). They, however, parametrically depend on two dimensionless numbers: the parameter of the horizontal elongation of the core (ν) and the parameter of the vertical flattening of the core (K):

$$\nu = \frac{a}{b}+\frac{b}{a}, \quad K = \frac{\tilde{c}}{\sqrt{ab}} = \frac{N_0}{f}\frac{c}{\sqrt{ab}}. \qquad (6)$$

Here, a,b are the horizontal semiaxes of the ellipsoid, c is the vertical semiaxis, and $\tilde{c}$ is the vertical axis $\tilde{c} = \frac{N_0}{f}c$ extended in $\frac{N_0}{f}$ times.

It should be noted that the constant characteristics of the eddy core $\mathrm{rot}_z\vec{u}$ and $\frac{\partial^2\psi}{\partial\tilde{z}^2}$ have the same sign, which coincides with the sign of potential vorticity of

the core σ, and are related by relation (2). This means that each expression $\frac{\mathrm{rot}_z\vec{u}}{\sigma}$ and $\frac{1}{\sigma}\frac{\partial^2\psi}{\partial\tilde{z}^2}$ changes in a range from 0 to 1 depending on the ν and K values. The increase in one parameter results in the decrease of another and vice versa. The redistribution of primary constant BV frequency (3), however, is related only to $\frac{\partial^2\psi}{\partial\tilde{z}^2}$ and does not depend on $\mathrm{rot}_z\vec{u}$. Thus, it should be expected that the deformation of the BV frequency would be stronger in eddies with a maximally high $\frac{1}{\sigma}\frac{\partial^2\psi}{\partial\tilde{z}^2}$ value. As would be shown below, this condition is implemented for thin axis-symmetrical eddies with $\nu = 2$ and $K \ll 1$.

The theory of ellipsoidal eddies applied here is based on two suggestions: homogenous potential vorticity of all particles of the eddy core σ and ellipsoidal morphology of the core. In reality, these properties of eddies are violated, however, the preservation of potential vorticity of particles (1) and (2) remains. This makes possible to consider the characteristics average by the eddy core volume $\mathrm{rot}_z\vec{u}$, $\frac{\partial}{\partial z}\frac{f^2}{N_0^2(z)}\frac{\partial\psi(x,y,z,t)}{\partial z}$ and σ, which are related by relation

$$\mathrm{rot}_z\vec{u} + \frac{\partial}{\partial z}\frac{f^2}{N_0^2(z)}\frac{\partial\psi(x,y,z,t)}{\partial z} = \sigma, \qquad (7)$$

where each sum in the left part of equation depends on the core morphology. Due to linearity of task (1) and (2) by σ, it should be expected that similar property would also be correct for the average $\mathrm{rot}_z\vec{u}$ and $\frac{\partial}{\partial z}\frac{f^2}{N_0^2(z)}\frac{\partial\psi(x,y,z,t)}{\partial z}$ values by the core volume. This allows the introduction of a dimensionless proportionality coefficient ε for $\frac{\partial}{\partial z}\frac{f^2}{N_0^2(z)}\frac{\partial\psi(x,y,z,t)}{\partial z}$ depending only on the core morphology (really depending on parameters ν and K):

$$\frac{\partial}{\partial z}\frac{f^2}{N_0^2(z)}\frac{\partial\psi(x,y,z,t)}{\partial z} = \varepsilon\sigma, \quad \mathrm{rot}_z\vec{u} = (1-\varepsilon)\sigma. \qquad (8)$$

The linear correlation between $\mathrm{rot}_z\vec{u}$ or $\frac{\partial^2\psi}{\partial\tilde{z}^2}$ and σ for ellipsoidal eddies follows directly from the solution of task (4)–(5) leading to the determination of ε as a function from ν and K:

$$\varepsilon = \frac{1}{2}K\int_0^\infty \frac{d\tilde{\mu}}{\left(K^2+\tilde{\mu}\right)^{\frac{3}{2}}\left(\tilde{\mu}^2+\nu\tilde{\mu}+1\right)^{\frac{1}{2}}}. \qquad (9)$$

The physical sense of parameter ε for both relations (8) and (9) is the same: it indicates the amount of the effect of vertical extension in a general law of conservation of potential vorticity. If ε is close to its maximum value of 1, the cores of these eddies should exhibit a strong change in the BV frequency. If ε is close to 0, no significant changes should be expected in the BV frequency in the eddy cores relatively to their background distributions. This is followed by the estimation of maximum possible BV frequencies in cyclones ($\sigma > 0$) $N^2_{\max} = N_0^2\left(1+\frac{\sigma}{f}\right)$ (hereinafter, for the simplicity, the BV frequency is termed by its square). The Rossby value $\mathrm{Ro} = \frac{|\mathrm{rot}_z\vec{u}|}{f} = \frac{(1-\varepsilon)\sigma}{f}$ in our approach should be low, which is correct at $\varepsilon \sim 1$ for thin eddies. As to the anticyclones ($\sigma < 0$), the expression for the minimum possible value of the BV frequency $N^2_{\min} = N_0^2\left(1-\frac{|\sigma|}{f}\right)$ indicates the presence of limitation $|\sigma| < f$ and possible achievement of fully homogeneous density core. The work [26] presents more detailed limitations for potential vorticity of the core σ of anticyclones taking into account the core morphology. These limitations on extremely possible BV frequencies $N^2_{\min}$ and $N^2_{\max}$ are deduced for the case of the absence of background currents (both barotropic and barocline). The consideration of barotropic currents will lead only to the change in multiplier σ to $(\sigma_{in} - \sigma_{out})$ in relations (4) and (5) and related formulas. Here, σ_{in} and σ_{out} are the potential vorticity of the core and the area beyond the core, respectively.

The theory also omits the possible water exchange between the eddy core and the ambient water area. In reality, both are present. All this could lead to strong reconstructions of the indicated frequencies $N^2_{\min}$ and $N^2_{\max}$. Thus, during the study of the real transformation of the BV frequency field by eddies, we will qualitatively take into account these limitations. In particular, it can be expected that the eddy cores of intense anticyclones would be fully homogeneous by density, whereas the isopycnals ejected from the core would form zones of significantly higher BV frequencies above and below the core. The conclusion for cyclones is more modest: the maximum BV frequency should increase with increasing intensity of the cyclone in the eddy cores and the $N^2_{\max}$ value is limited from the top.

Relation (3) is the field of $N^2(x,y,z,t)$ which is primarily constant BV frequency N_0^2 deformed by eddy $N^2(x,y,z,t)$ in the absence of external background currents. In case of ellipsoidal eddies and the same conditions, relation (3) is transformed into precise expression

$$N^2 = N_0^2\left\{1+\frac{\varepsilon}{1-\varepsilon}\frac{\mathrm{rot}_z\vec{u}}{f}\right\} = N_0^2\left\{1+\mathrm{sign}(\sigma)\frac{\varepsilon}{1-\varepsilon}\mathrm{Ro}\right\}, \quad (10)$$

where parameter ε is determined by equation (9) and a new BV frequency N^2 is constant. In case of the eddy with oval core and a more complex distribution of the potential vorticity of the core, this formula can be used for the estimations of eddy characteristics with Rossby number $\mathrm{Ro} = \frac{|\mathrm{rot}_z\vec{u}|}{f}$. Formula (10) allows the determination of parameter ε from natural data by measured fields of BV frequency N^2, N_0^2 and Ro and, therefore, finding a contribution, which makes an effect of vertical extension of elementary liquid volumes into potential vorticity of the core. In turn, the knowledge of ε allows the estimations of the parameter of vertical flattening of the core K.

In this work, we will calculate the distribution of potential vorticity in eddies by natural data using a suggestion on constant N_0 and variable $N(z)$ of the BV frequency by formulas (1) and (2). The discussion of this approach in estimation of the term $\frac{1}{f}\frac{\partial}{\partial z}\frac{f^2}{N_0^2(z)}\frac{\partial\psi(x,y,z,t)}{\partial z}$ is given below. The work [26] discussed the estimation of the same term by comparison of vertical distributions of the density field in the eddy core and a calm zone, where the movement of water can be omitted. This results in two useful ratios. In first case, simple estimation of the term $\frac{1}{f}\frac{\partial}{\partial z}\frac{f^2}{N_0^2(z)}\frac{\partial\psi(x,y,z,t)}{\partial z}$ can be calculated for the chosen horizon:

$$\frac{1}{f}\frac{\partial}{\partial z}\frac{f^2}{N_0^2(z)}\frac{\partial\psi(x,y,z,t)}{\partial z} = \frac{N^2(x,y,z,t)-N_0^2(z)}{N_0^2(z)} - \frac{g}{\rho_*}(\rho(x,y,z,t)-\rho_0(z))\frac{\partial}{\partial z}\left\{\frac{1}{N_0^2(z)}\right\}, \quad (11)$$

where $N^2(x,y,z,t)$ is the distribution of the squared BV frequency in the eddy influence zone, $N_0^2(z)$ is the profile of the squared BV frequency beyond the eddy influence zone (background BV frequency), $\rho(x,y,z,t)$ is the current value of full density in a considered point, $\rho_0(z)$ is the density of water at rest at the same horizon (background), and ρ_* is the average density of water (1028 km/m^3 in calculations).

In second case, the calculation of the average value $\frac{1}{f}\frac{\partial}{\partial z}\frac{f^2}{N_0^2(z)}\frac{\partial\psi(x,y,z,t)}{\partial z}$ by a liquid layer between the depths h_1 and h_2 results in the following relation:

$$\left\langle\frac{1}{f}\frac{\partial}{\partial z}\frac{f^2}{N_0^2(z)}\frac{\partial\psi(x,y,z,t)}{\partial z}\right\rangle_{h_1}^{h_2} = -\frac{g}{\rho_*}\frac{1}{h_2-h_1}\left\{\frac{1}{N_0^2(h_2)}(\rho(x,y,h_2,t)-\rho_0(h_2)) - \frac{1}{N_0^2(h_1)}(\rho(x,y,h_1,t)-\rho_0(h_1))\right\}, \quad (12)$$

which contains no derivatives and all parameters in the right part are easily calculated from natural data. Then, the substitution of expression (12) to formula (7) results in the final formula for the calculation of potential vorticity by Rossby:

$$\sigma = \langle\mathrm{rot}_z u\rangle_{h_1}^{h_2} - f\frac{g}{\rho_*}\frac{1}{h_2-h_1}\left\{\frac{1}{N_0^2(h_2)}(\rho(x,y,h_2,t)-\rho_0(h_2)) - \frac{1}{N_0^2(h_1)}(\rho(x,y,h_1,t)-\rho_0(h_1))\right\}. \quad (13)$$

3. DATA

We used the GLORYS12V1data available from the website of the Copernicus Marine Environment Monitoring Service (CMEMS) (http://marine.copernicus.eu). GLORYS12V1 is a global oceanic eddy-resolving reanalysis, which is based on the NEMO model elaborated using ECMWF ERA-Interim atmospheric reanalysis. The initial conditions for temperature and salinity were taken from EN.4.2.0 Hadley Center data for 1991. An unquestionable advantage of the GLORYS12V1 reanalysis is the assimilation of satellite and in situ data. In particular, more than 5000 profiles of Argo floats are assimilated in this product, as well as along-tracking anomalies of the sea level (SLA, Sea Level Anomalies), sea surface temperature (SST), and temperature and salinity profiles from the CMEMS CORAv4.1 database beginning from 2005. The Kalman filter is used for assimilation. The data on temperature and salinity at 50 horizons with a spatial resolution of 1/12° (~4 × 8 km for high latitudes) are daily and monthly renewed. For verification, we used data from 50 horizons for June 10, 2010.

The profiles of the BV frequency were calculated using thermodynamic equation TEOS-10 [18] in Matlab. The potential vorticity was calculated from formula (1). Although frequency N^2 occurs in denominator, it makes no difficulties in calculations, because the BV frequency values close to 0 are present only in

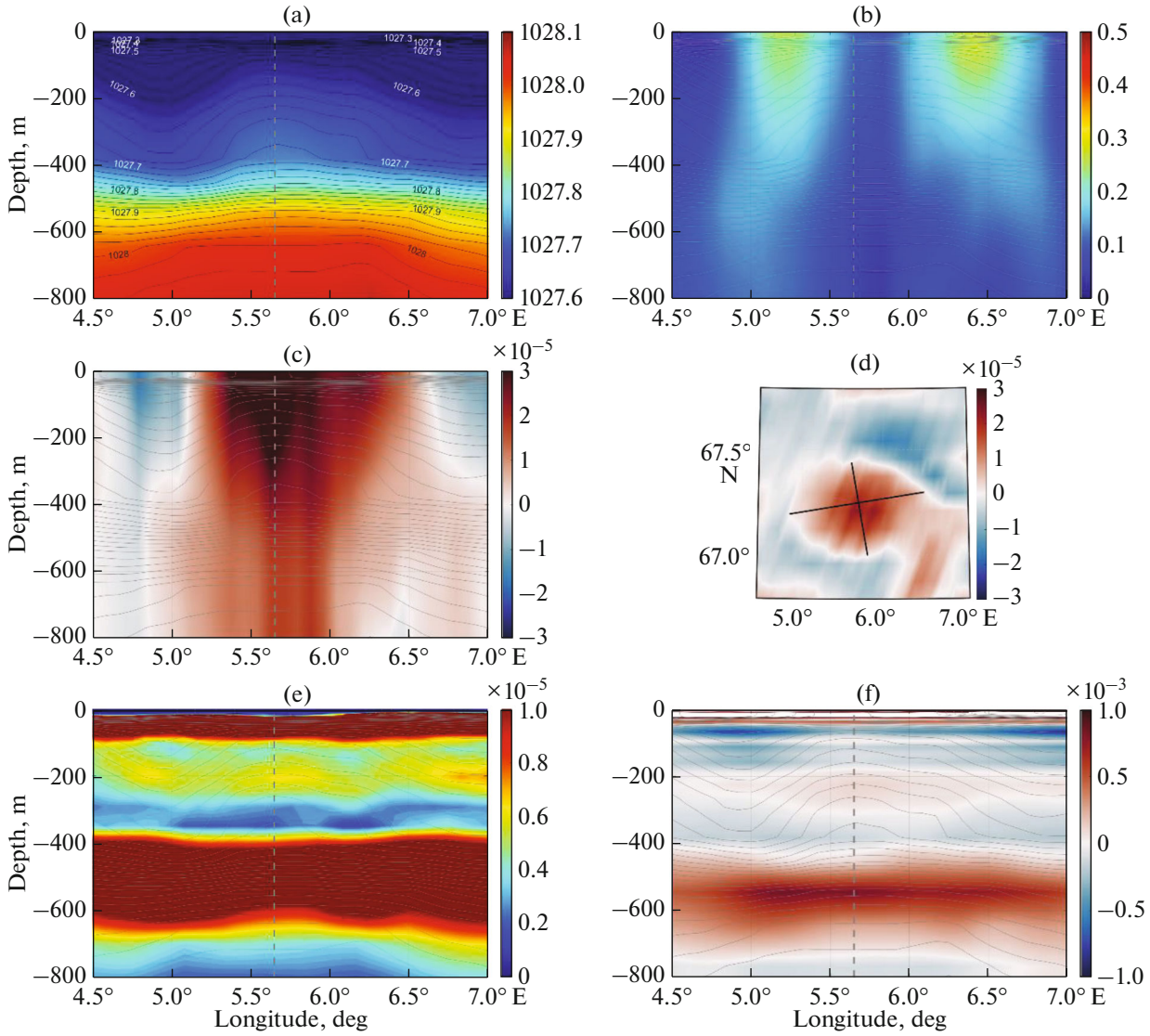

Fig. 3. Cyclone: potential density, kg/m^3 (a); orbital velocity, m/s (b); relative vorticity rot$_z\vec{u}$, s^{-1} (c); relative vorticity at 417 m horizon, the axes of ellipsis are shown by black lines (d); squared BV frequency, s^{-2} (e); potential vorticity σ, s^{-1} (f). Gray lines show isopycnals. The vertical dotted line marks the eddy center. The vertical sections are through 67.25° N. Gray dotted line occurs through the eddy center.

the upper quasi-homogenous layer and zero values are absent.

4. MAIN CHARACTERISTICS OF THE CYCLONE

It is seen from Fig. 3a that the cyclone analyzed (Fig. 2b) is subsurface and the submergence of isopycnals to the surface reaches 100 m in a layer of ~450 m. The dynamic signal of the eddy identified at orbital velocities is also typical of the deeper layers (>1000 m). The orbital velocities in the cyclone reach 30 cm/s (Fig. 3b). The maximum values of relative vorticity rot$_z\vec{u}$ are registered up to 500 m (Fig. 3c). At the 417 m horizon, the spatial scales of the cyclone, which are determined by the boundary with zero relative vorticity, are 72.3 km of the length and 48.8 km of the width with an effective horizontal size $L_{\text{eff}} = \sqrt{ab} = 59.4$ km (Fig. 3d) [4]. The potential vorticity σ has the maximum values of 1.0×10^{-3} s^{-1} in the area of the isopycnic concentration below the cyclonic core and, partly, in the upper subsurface layer. The maximum changes in the BV frequency correspond to the layer of 100–400 m (Fig. 3e). Two areas of the concentration of the isopycnals in the upper layer and at a depth of 400–600 m correspond to two areas of the higher N^2 values. The σ values below the subsurface layer are negative; both positive and negative extreme values in figure are 1.0×10^{-4} s^{-1} (Fig. 3f). It is evident that the

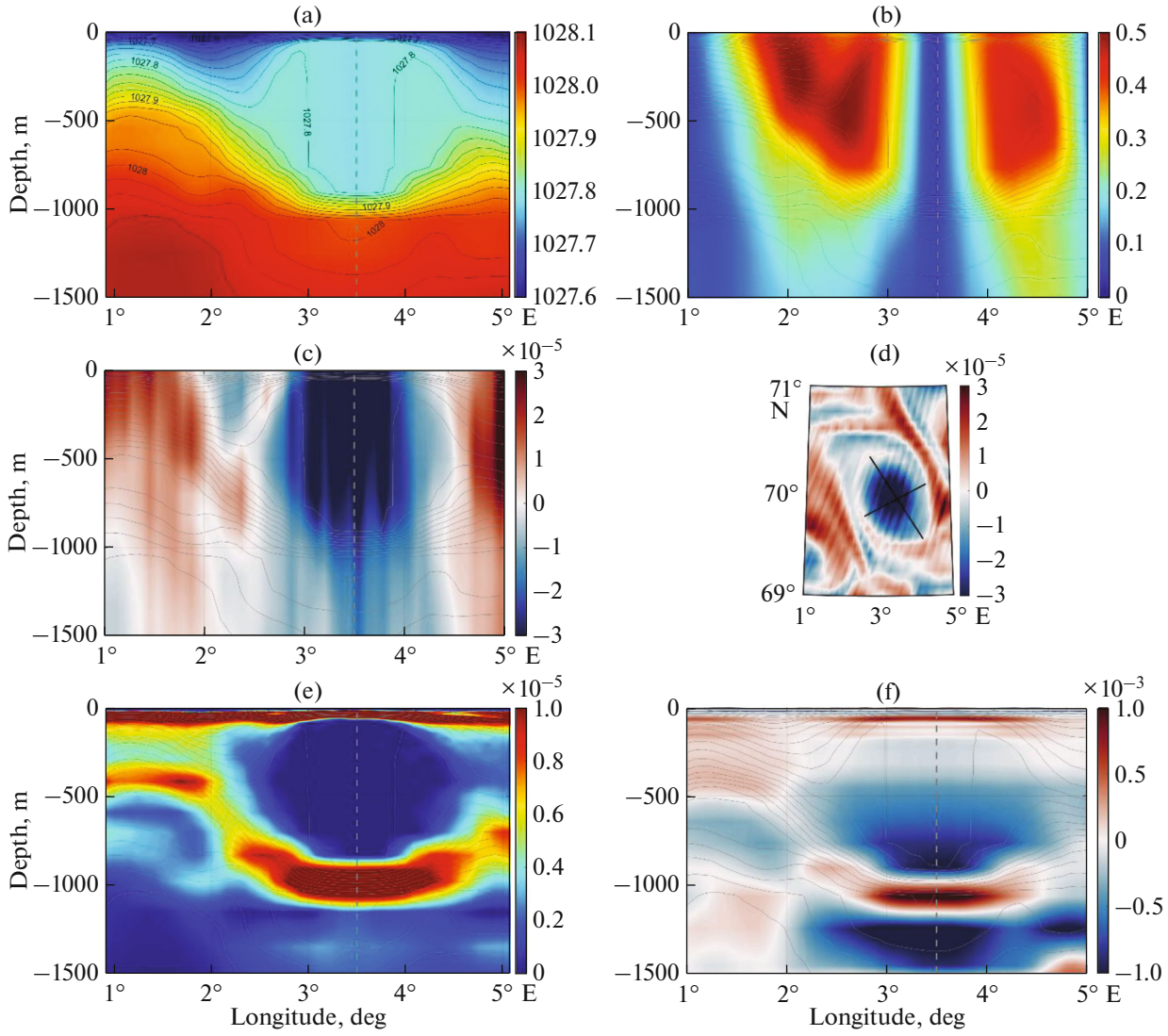

Fig. 4. Anticyclone: (a), (b), (c), the vertical sections of fields of potential density (kg/m^3), orbital velocity (m/s), and relative vorticity $\mathrm{rot}_z\vec{u}$ (s^{-1}), respectively, through the anticyclone axis; (d) horizontal section at a depth of 417 m of relative vorticity, the ellipsis axes are shown by black lines; (e) squared BV frequency, s^{-2}; (f) potential vorticity σ, s^{-1}. Gray lines are shown by isopycnals. The vertical sections are shown through 67.25° N. Gray dotted line through the eddy center.

main contribution into σ value is provided by the term

$$\frac{\partial}{\partial z}\frac{f^2}{N_0^2(z)}\frac{\partial\psi(x,y,z,t)}{\partial z}.$$

5. MAIN CHARACTERISTICS OF THE ANTICYCLONE

The Lofoten anticyclonic eddy is a strong dynamic event (Fig. 4a), the dynamic signal of which is propagated to the seafloor [25]. The change in thermohaline characteristics is mostly noted in a layer up to 1000 m and the core is located in a layer of 100–800 m. In works [1, 2, 23], the position of the core was noted at a depth of 200–800 m. The orbital velocities in the anticyclone exceed 50 cm/s (Fig. 4b). The relative vorticity is maximum (by the module) in the core (Fig. 4c), but the dynamic signal (negative values of the relative vorticity) is traced to the seafloor (3250 m). Figure 4d shows that the scales of the anticyclone significantly exceed those of the cyclone both along the vertical and horizontal (a = 108.7 km, b = 67.9 km) with an effective horizontal size $L_{\mathrm{eff}} = \sqrt{ab}$ = 85.9 km. The eddy core is well distinguished in the section of the BV frequency (Fig. 4e); the BV frequency values in the layers above and below the core with concentration of isopycnals are positive and maximum and are zero in the core. The section of potential vorticity (Fig. 4f) is similar to the plot of the BV frequency, whereas the max-

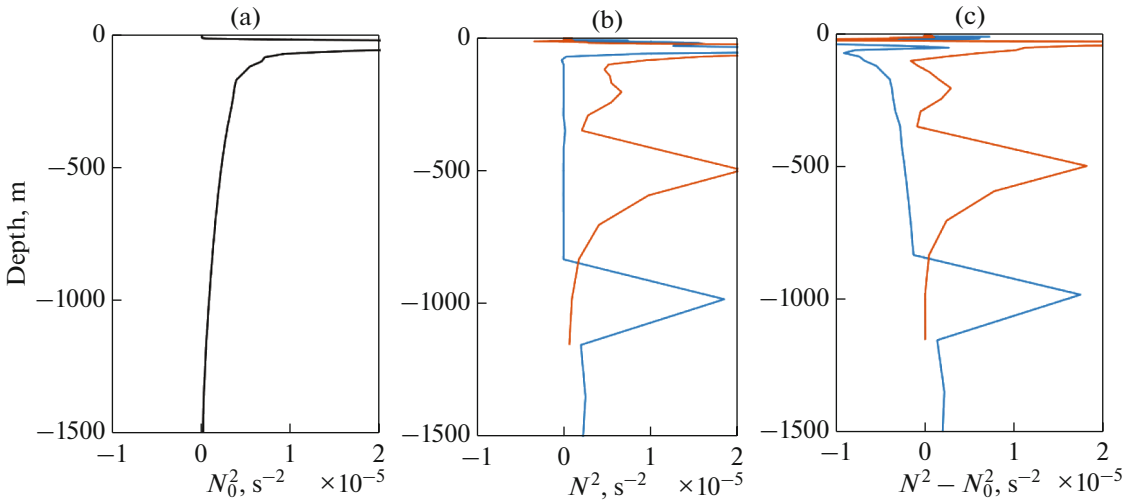

Fig. 5. Profiles of squared BV frequency, s^{-2}: (a) background $N_0^2(z)$; (b) $N^2(z)$ in the center of the eddy; (c) anomalies $N^2(z) - N_0^2(z)$ in the center of the eddy. Orange and blue lines belong to the cyclone and anticyclone, respectively.

imum positive σ values correspond to the areas of the concentration of isopycnals and reach 1.0×10^{-3} s^{-1}. The maximum negative values (-1.0×10^{-3} s^{-1}) occur in adjacent layers. The comparison of sections of $\mathrm{rot}_z\vec{u}$ and σ shows that the main contribution into σ value is provided by the term $\frac{\partial}{\partial z}\frac{f^2}{N_0^2(z)}\frac{\partial \psi(x,y,z,t)}{\partial z}$.

The presence of a "column" of rotating liquid below the eddy cores are noteworthy in study of fields of relative vorticity of the cyclone and anticyclone. It is evident from Figs. 3c and 4c. Judging from that the "columns" are extended from the lower boundary of the eddy cores to the seafloor, it can be concluded on barotropic origin of this event. It is likely that these "rotating columns" formed as a result of oceanic response to the sea surface level curved by eddies and incomplete compensation of these velocities by the displacement of isopycnals in the water column.

6. BRUNT–VÄISÄLÄ FREQUENCY PROFILES

The profiles of the BV frequency in eddies and corresponding anomalies relatively background frequency are shown in Fig. 5. It is evident that the extremes are reached in an upper 50-m layer. A maximum of anomalies of the BV frequency with positive values is registered in the cyclonic core in a layer of 100–400 m. This is related to the bending isopycnals to the surface. Another maximum is located at the 500 m horizon, which exhibits the concentration of isopycnals (Fig. 5b). In the cyclonic core (a layer of 200–300 m), the anomalies of the BV frequency are positive relatively to the background values (Fig. 5c). It should be noted, however, that the cyclonic core contains both positive and negative anomalies with dominant positive ones.

In the anticyclonic core (Fig. 5c), the vertical changes in the BV frequency are almost absent, because the core is almost homogenous by density (see also Fig. 4e) and the anomalies of the BV frequency are negative relatively to the background frequency (Fig. 5c). If we consider the fine details of the BV frequency in the anticyclonic core, it should be noted that the core consists of two layers almost homogeneous by density, each of which is characterized by relatively low oscillations of the BV frequency: $\left|\frac{N^2(x,y,z,t)}{N_0^2(z)}\right| < 0.01$. This inequality is violated in the area of the 350 m horizon: $\frac{N^2(x,y,z,t)}{N_0^2(z)} \approx 0.05$, which indicates a weak density jump. The average value of relative oscillations of the BV frequency, however, will remain in the same range: $\left|\frac{N^2(x,y,z,t)}{N_0^2(z)}\right| < 0.01$.

Thus, the BV frequency in the cyclonic core increases on average in contrast to its decrease in the anticyclonic core to complete homogeneity by density.

7. PARAMETER OF VERTICAL FLATTENING OF THE EDDY CORE ACCORDING TO THE THEORY OF ELLIPSOIDAL VORTICES

According to relations (23) [26], Fig. 6 shows the correlation between dimensionless velocity rotor $\frac{\mathrm{rot}_z\vec{u}}{\sigma}$ and parameter K, which is the vertical distance from

axis K to line $\frac{\mathrm{rot}_z\vec{u}}{\sigma}$ for the axis-symmetrical eddies. In the same figure, the dimensionless value $\frac{1}{\sigma}\frac{\partial^2\psi}{\partial\tilde{z}^2}$ is the vertical distance from line $\frac{\mathrm{rot}_z\vec{u}}{\sigma}$ to 1. In the previously accepted symbols, $\frac{1}{\sigma}\frac{\partial^2\psi}{\partial\tilde{z}^2} = \varepsilon$ and $\frac{\mathrm{rot}_z\vec{u}}{\sigma} = 1-\varepsilon$. As seen, both values $\frac{\mathrm{rot}_z\vec{u}}{\sigma}$ and $\frac{1}{\sigma}\frac{\partial^2\psi}{\partial\tilde{z}^2}$ are 1 in total. For small values $0 < K < 0.6$, the term $\frac{1}{\sigma}\frac{\partial^2\psi}{\partial\tilde{z}^2}$ is dominant and, for the higher values ($K > 0.6$), the term $\frac{\mathrm{rot}_z\vec{u}}{\sigma}$ is more significant; it is evident that they are the same at $K \cong 0.6$. This means that a significant reconstruction of the density field should be observed in fine eddies. Nonetheless, the thickness of anticyclones is limited by $\varepsilon < \frac{1}{1+\mathrm{Ro}}$. In our case, $\mathrm{Ro} = 0.3$, thus this condition for parameter ε yields the numerical value of <0.77, which can be recalculated to parameter K by the given plot yielding the limitation of $K > 0.18$, which means that the anticyclone cannot be extremely thin. In a general case, the maximum value of parameter K_0 related to the maximum value $\varepsilon_0 = \frac{1}{1+\mathrm{Ro}}$ depends on the Rossby value $K_0 = K_0(\mathrm{Ro})$ and can be interpreted as a limitation for the thickness of the anticyclonic core $\frac{N_0}{f}\frac{c}{\sqrt{ab}} > K_0$. At maximum values $\varepsilon = \varepsilon_0$ (or $K = K_0$), the anticyclonic core becomes fully homogeneous by density along the vertical. The condition $\frac{N_0}{f}\frac{c}{\sqrt{ab}} > K_0$ is equal to stability of stratification in the eddy core at a certain Rossby value Ro. There are no similar limitations for the cyclone.

The parameter of flattening of the cores is calculated for eddies, the location of which is shown in Fig. 2 [26]. The average BV frequencies are $N_0 = 2.59\times10^{-3}$ s^{-1} and $N_0 = 2.06\times10^{-3}$ s^{-1} for the cyclone and anticyclone, respectively (Fig. 5). The parameters of vertical flattening are $K = 0.13$ and $K = 0.15$ for the cyclone and anticyclone, respectively. Both values correspond to thin eddies in our classification. It should be noted that, the limitation for parameter $K > K_0 = 0.18$ is fulfilled for the anticyclone (with a small error). This can be related to that the limitation $K > K_0$ is yielded assuming the axis-symmetrical eddy, i.e., the parameter of horizontal elongation of the core $\nu = 2$. In our case, the eddy is asymmetrical and, for the anticyclone, this parameter is slightly higher $\nu = 2.2$. According to (5), the asymmetry leads to decreasing K_0 value that approaches K_0 to 0.15. The main reason of the different estimation of K, however, lies in that the upper boundary of the eddy core occurs closely to the surface or even touches it. The correction of K values taking into consideration the closeness of the core to the sea surface will be suggested below.

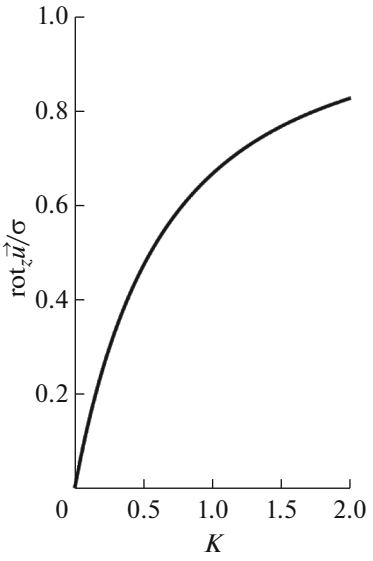

Fig. 6. Correlation between dimensionless parameter $\frac{\mathrm{rot}_z\vec{u}}{\sigma}$ and parameter of vertical flattening K for axis-symmetrical eddies. At $K = 0$ $\frac{\mathrm{rot}_z\vec{u}}{\sigma} = 0$, at $K \to \infty$ $\frac{\mathrm{rot}_z\vec{u}}{\sigma} \to 1$.

8. APPLICATION OF THE IMAGE METHOD TO ANALYZED EDDIES

Application of the image method to analyzed eddies indicates that the presence of the sea surface should lead to a real increase in parameter K, but no more than twice. As a result, a range of an effective value of vertical flattening for the cyclone and anticyclone will be $0.13 < K < 0.26$ and $0.15 < K < 0.30$, respectively. If the real K value will be close to the left limit of inequalities, the sea surface impact could be ignored. If it will be closer to the right one, the sea surface impact on the reconstruction of the density field in the eddy cores will be significant.

The image method is physically used as a substitution of the approximation of the "solid cap" on the sea surface, according to which the vertical movements are absent on the sea surface. In reality, the sea surface is deformed under water movement and this, in particular, can be registered on altimetric maps. The image method ignores the curve of free surface below the subsurface eddy and this leads to the barotropic

response along the entire sea depth. On horizons below the eddy cores, we really observe the "column" of vorticity, which is stable moving down from the eddy core. The effect of the "vorticity column" can decrease or even dissipate in case of the formation (due to some reasons) of curving isopycnals of opposite direction below the sea surface than on the sea surface. This effect is currently unstudied for our polygon and requires description in model and natural studies.

9. EXPERIMENTAL DETERMINATION OF COEFFICIENT ε AS A CONTRIBUTION OF EXTENSION EFFECT TO THE POTENTIAL VORTICITY OF THE CORE. INDIRECT DETERMINATION OF THE PARAMETER *K*

Let us derive from the working formula (10) for the constant background BV frequency N_0^2. Knowing N^2, N_0^2, and Ro, we can determine parameter ε. In reality, N_0^2 and N^2 depend on the profile coordinates and the core morphology differs from ellipsoidal. Let us suggest that the estimation of Ro is correct for the entire core volume as also the found parameter ε. In this case, we consider a more complex scenario explained in section 2.4 of the first paper [26] (the core with complex interiors). Formula (10) results in relation

$$N^2 - N_0^2 = N_0^2 \operatorname{sign}(\sigma)\frac{\varepsilon}{1-\varepsilon}\mathrm{Ro}.$$

Integrating this relation by z from the sea surface $z = 0$ to the depth H, we obtain a link between integral characteristics

$$\int_0^H (N^2 - N_0^2)dz = \operatorname{sign}(\sigma)\frac{\varepsilon}{1-\varepsilon}\mathrm{Ro}\int_0^H N_0^2 dz,$$

which can be interpreted as a correlation of average values by the thickness of integration H:

$$\left\langle N^2 - N_0^2 \right\rangle = \left\langle N_0^2 \right\rangle \operatorname{sign}(\sigma)\frac{\varepsilon}{1-\varepsilon}\mathrm{Ro}.$$

Figure 7 shows the plots $\left\langle N^2(z) - N_0^2(z)\right\rangle$ and $\delta(z) = \dfrac{\left\langle N^2(z) - N_0^2(z)\right\rangle}{\left\langle N_0^2(z)\right\rangle}$. In contrast to parameter $\delta = \dfrac{N^2 - N_0^2}{N_0^2}$ (see [26]), which is calculated for the case of the constant background BV frequency N_0^2, the relative change in the BV frequency is considered a function of the averaging depth. Averaging is conducted in a layer-by-layer manner from the surface to a certain depth: first, upper layer, then two upper layers, then three upper layers, etc. to the depths below the boundary of the eddy cores. It is seen that, beginning from the depths of 50 m, the $\delta(z)$ values for the cyclone and anticyclone are smooth monotonous functions, which weakly depend on the lower depth of occurrence of the eddy core. For the depths of 50–417 m (approximately the position of the cyclone core), parameter $\delta(z)$ is 0.5. This means that the average changes of the squared BV frequency induced by the eddy compose 50% of the average square of the background BV frequency along the thickness of the cyclone core. This also means that stratification increases in the cyclone inside the core at $\delta = 0.5$ and $N^2(z) \approx 1.5N_0^2(z)$ is approximately fulfilled.

According to Fig. 7b, parameter $\delta(z)$ is $\delta = -0.69 \approx -0.7$ for the averaging horizons from 50 to 833 m for the anticyclone. Unfortunately, at this approach, we observed a strong correlation between parameter δ and the depth of occurrence of the upper layer boundary. For example, if we consider the averaging layer from 100 to 833 m, this parameter will increase by absolute value to $\delta \approx -0.9$. Qualitatively, this means that the relative change in the squared BV frequency in the anticyclonic core is high. Liquid in the anticyclonic core becomes more homogeneous by density. The last estimations for the squared BV frequency are calculated using natural data assuming a suggestion on the constant background BV frequency and correct theory of ellipsoidal eddies. In reality, this theory can be very rough for the case of variable background BV frequency. For the quantitative estimation in this case, we will use the consequence from equation (11) ignoring the second term, which is low according to Fig. 7. Then,

$$\frac{1}{f}\frac{\partial}{\partial z}\frac{f^2}{N_0^2(z)}\frac{\partial\psi(x,y,z,t)}{\partial z} \approx \frac{N^2(x,y,z,t) - N_0^2(z)}{N_0^2(z)}. \quad (14)$$

Both on the cyclone and anticyclone axes, the uppermost oceanic layer to a depth of 50 m exhibits the high values of parameter $\dfrac{N^2(x,y,z,t) - N_0^2(z)}{N_0^2(z)}$ related to a significant change in frequency $N^2(x,y,z,t)$ in this layer relatively to its background value $N_0^2(z)$. The implementation of a correlation similar to (13) should be expected in the upper 50-m layer. Thus, taking note of the experimental fact of high values $N^2(x,y,z,t)$, we ignore this layer in our discussion. Nonetheless, approaching top to bottom to the 50 m horizon on the anticyclone axis, there is a sharp decrease in parameter $\dfrac{N^2(x,y,z,t) - N_0^2(z)}{N_0^2(z)}$, which becomes 0 for a horizon of ≈50 m.

At depths of 50–100 m, parameter $\dfrac{N^2(x,y,z,t) - N_0^2(z)}{N_0^2(z)}$ for the anticyclone becomes

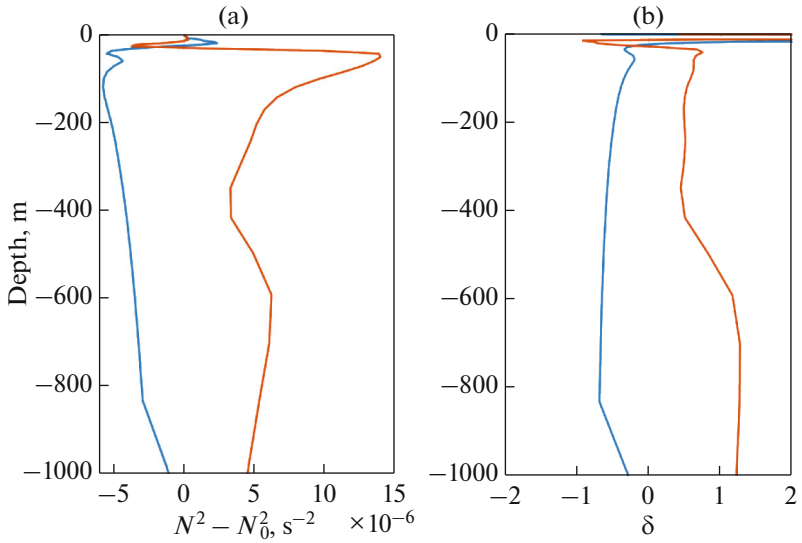

Fig. 7. Layer-by-layer averaged characteristics $\left\langle N^2 - N_0^2 \right\rangle$ (a) and $\delta = \dfrac{\left\langle N^2 - N_0^2 \right\rangle}{\left\langle N_0^2 \right\rangle}$ (b) for the cyclone (orange lines) and anticyclone (blue lines).

negative and reaches −1 at the 100 m horizon. Below this depth to the 803 m horizon, this parameter remains close to −1 (with an accuracy of no less than 1%) that means almost complete homogeneity of density in the eddy core excluding a fine layer at a depth of 350 m, where we observe a small peak of BV frequency or, what is the same, a small jump in the vertical distribution of the density field. This can be interpreted as follows: the anticyclone core is composed of two layers of liquid homogeneous by density with poorly distinct density values in each layer. Because the difference in density is small, then, the anticyclonic core can approximately be considered completely homogenous by density.

Thus, the anticyclonic core is almost homogenous by density with a numerical estimation of the average square of BV frequency of the core $\left\langle \dfrac{N^2(x,y,z,t)}{N_0^2(z)} \right\rangle < 0.01$. This inequality is fulfilled locally in all horizons of the eddy core of the anticyclone except for a small layer in the area of a depth of 350 m. The squared BV frequency of the anticyclone core is estimated as

$$\left\langle N^2(x,y,z,t) \right\rangle \approx 0.01 \left\langle N_0^2(z) \right\rangle. \quad (15)$$

As for the fine effects in the cyclonic core, according to Fig. 8, the term describing the extension effect (13) with a variable BV frequency has a variable sign with a positive average value on the thickness of the core, which is interpreted as a complex eddy integrally representing the cyclone. The average value of parameter $\dfrac{N^2(x,y,z,t) - N_0^2(z)}{N_0^2(z)}$ in terms of the 100–433 m horizons of the cyclone core is estimated as $\left\langle \dfrac{N^2(x,y,z,t) - N_0^2(z)}{N_0^2(z)} \right\rangle \approx 0.4$, which yields an approximate correlation of induced and background BV frequencies

$$\left\langle N^2(x,y,z,t) \right\rangle \approx 1.4 \left\langle N_0^2(z) \right\rangle. \quad (16)$$

Relation (15) almost coincides with similar relation $N^2(z) \approx 1.5\ N_0^2(z)$, which was calculated using hardest condition (constant BV frequency). For clarity, we will further consider that $N^2(z) \approx 1.5 N_0^2(z)$. Below the eddy core of the anticyclone, the BV frequency increases and becomes much higher than the background value; above and below the anticyclonic core, the isopycnals are concentrated pushing from the core. As a result, there is an increased (relatively to the background) BV frequency value above and below the core, thus, the increase in potential vorticity of particles of these zones.

Thus, we used two approaches in estimation of the contribution of extension effect into potential vorticity of liquid particles (in fact, estimation of the second term in equation (1)). The first more rough approach uses the constant background BV frequency and then, considering that the frequency is variable, we averaged the result by the thickness of the core. This approach actively uses the analytical theory of ellipsoidal eddies. At the second approach, the BV frequency was free from any limitations and the second term was calculated directly from natural data. The second approach is more physical, but it is devoid of a possible substan-

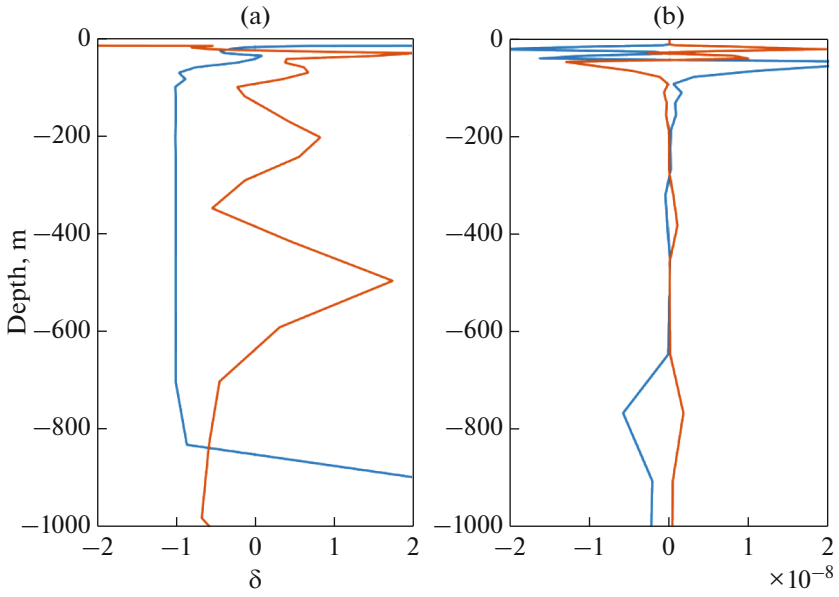

Fig. 8. $\frac{N^2(x,y,z,t)-N_0^2(z)}{N_0^2(z)}$ (a) and $\frac{g}{\rho_*}(\rho(x,y,z,t)-\rho_0(z))\frac{\partial}{\partial z}\left\{\frac{1}{N_0^2(z)}\right\}$ (b) as a function of depth z for the cyclone (orange lines) and anticyclone (blue lines).

tiated use of analytical results, because there is no corresponding theory for the general case. As was shown by calculations, both approaches yield qualitatively similar results. For quantitative estimation of a significance of extension effect in potential vorticity of liquid particles of the eddy cores, however, we should use a more precise approach (13).

The contribution of the extension effect to potential vorticity of the cyclone $\varepsilon = 0.63$ can be estimated by value $\delta = 0.5$ and Rossby number $\mathrm{Ro} = 0.3$ from equation $\varepsilon = \frac{\delta}{\mathrm{Ro}+\delta}$. Thus, the rotation provides the remaining 37%. As seen, the role of both effects is significant, but the extension effect is more important.

For qualitative estimation of the parameter of vertical flattening K of the cyclonic core, let us use the correlation between $\frac{1}{\sigma}\mathrm{rot}_z\vec{u}$ and K (Fig. 6). Value $\frac{1}{\sigma}\mathrm{rot}_z\vec{u} = 0.37$ corresponds to value $K = 0.26$ (effective parameter of vertical flattening). Comparing it with a range of $0.13 < K < 0.26$, which was directly calculated using a correction for the presence of free sea surface, we concluded that the sea surface strongly affected the reconstruction of the density field in the cyclonic core, because the effective value of parameter $K = 0.26$ coincides with the right boundary of the range.

Similar work by natural data for the anticyclone shows that value $\varepsilon = 0.70$ corresponds to the relative change in BV frequency $\delta = -0.7$ and $\mathrm{Ro} = 0.3$ in the anticyclone. The effective parameter of vertical flattening for the anticyclone is estimated at $K = 0.34$. A range of values K from the theory of ellipsoidal eddies taking into account the sea surface effect is $0.15 < K < 0.30$. The limitations from stability conditions of stratification are as follows: $\varepsilon < 0.77$ and $K > K_0 = 0.18$; rounding to the tens portions will yield $K_0 = 0.2$.

The entire theory, which is the basis for our consideration, is intended for the processes with low Rossby numbers Ro. This means that the geostrophic component of velocities is 0.7 from the total velocity, whereas 30% are the ageostrophic velocities, which are absent in theory, however, they can be present in natural data. It is reasonable to suggest that the accuracy of the theory by velocities in general is also ~30%. Thus, all numerical results by velocities, which differ by less than 30%, should be interpreted as coinciding. To remove this inconsistency, let us round these numbers to tens portions. As a result, the parameters of vertical flattening for the cyclone and anticyclone will coincide: $K = 0.3$. The limitation for K for the anticyclone is implemented, because $K_0 = 0.2$.

10. CONCLUSIONS

In this article, we studied the role of the BV frequency in mesoscale eddies. Two eddies of the Lofoten Basin of the Norwegian Sea (cyclone and anticyclone) are considered with the example of GLORYS12V1 oceanic reanalysis data. For these eddies, the vertical sections of potential density and BV frequency are

plotted, the scales and orbital velocities are calculated, the distribution of the BV frequency in the core and its anomalies relatively to the background BV frequency and the plots of relative and potential vorticity are plotted. Analysis of these results allowed following conclusions.

The orbital velocities in the cyclone reach 30 cm/s, whereas the spatial longitudinal and transverse scales are 72.3 and 48.8 km, respectively. The orbital velocities in the anticyclone exceed 50 cm/s (maximum value of 50.8 cm/s), whereas the spatial longitudinal and transverse scales are 108.7 and 67.9 km, respectively.

Isopycnals in cyclones and anticyclones are deformed on average in opposite directions. The cyclonic eddies make isopycnals closer pulling the closest external isopycnals inside the eddy core, whereas the ancticyclone eddies push apart the isopycnals from each other. The latter leads to the increase in the BV frequency in the cyclonic eddy core and its corresponding decrease in the anticyclone. It is shown that the anomalies of the BV frequency relatively to the background frequency are positive and negative in the core of the cyclone and anticyclone, respectively. The relative changes in the squared BV frequency are significant: ~50 and 99% for the cyclone and anticyclone, respectively. Theoretical substantiation of this fact is described by formula (10) of the first part of the work [26]. Figure 5c also confirms this conclusion.

The effective reconstruction of the BV frequency occurs exclusively in fine eddies with small parameters of vertical flattening of the core K. For the anticyclone, there is a limitation from the bottom by number $K > K_0$. Critical K_0 is related to the dimensionless geometrical parameters of the eddy core and the squared BV frequency value average by vertical. According to theoretical calculations and estimations by natural data, the coinciding values of these parameters are obtained both for cyclone and anticyclone $K = 0.3$ and $K_0 = 0.2$.

The potential vorticity calculated by formula (1), as well as the relative vorticity, is well distinguished in the eddy cores and are traced in eddies to the bottom (both in cyclone and anticyclone).

The position of the eddy cores near the sea surface leads to that the sea surface significantly affects the dynamics of eddies that, in turn, is reflected in the increasing effective value of the parameter of vertical flattening of the eddy cores (approximately, in two times).

ACKNOWLEDGMENTS

We are grateful to members of the Scientific Council of the Institute of Oceanology, Russian Academy of Sciences for discussion of this work.

FUNDING

This work was supported by the Russian Science Foundation (project no. 22-27-00004) and state contract no. 0128-2021-0002.

REFERENCES

1. T. V. Belonenko, D. L. Volkov, Yu. E. Norden, and V. K. Ozhigin, "Circulation of waters in the Lofoten Basin of the Norwegian Sea," Vest. St. Petersburg. Univ. **7**, 108—121 (2014).
2. T. V. Belonenko, A. V. Koldunov, E. A. Sentyabov, and A. l. Karsakov, "Thermohaline structure of the Lofoten vortex in the Norwegian sea based on field research and hydrodynamic modeling," [In Russian]. Vestn S. Petersbur. Un-ta, Earth sciences. **63** (4), 502—519 (2018). https://doi.org/10.21638/spbu07.2018.406
3. V. V. Zhmur, *Mesoscale Oceanic Eddies* (GEOS, Moscow, 2011) [in Russian].
4. V. V. Zhmur, E. V. Novoselova, and T. V. Belonenko, "Potential Vorticity in the Ocean: Ertel and Rossby Approaches with Estimates for the Lofoten Vortex," Izvestiya, Atmospheric and Oceanic Physics. **57** (6), 632—641 2021. https://doi.org/10.31857/S0002351521050151
5. V. V. Zhmur and K. K. Pankratov, "Dynamics of ellipsoidal near-surface vortex in a nonuniform stream," Okeanologiya **29**, 205—211 (1989).
6. V. V. Zhmur and A. F. Shchepetkin, "Evolution of the ellipsoidal vortex in stratified ocean in the f-plane approximation," Izv. RAN. Fizika atmosfery i okeana **27**, 492—503 (1991).
7. A. V. Koldunov and T. V. Belonenko, "Hydrodynamic simulation of the vertical speed field in the Lofoten vortex," Izv. RAN. Fizika atmosfery i okeana **56**, 575—585 (2020). https://doi.org/10.31857/S0002351520040045
8. L. M. Naumov and S. M. Gordeeva, "Lateral transport of heat and salt in the Lofonten Basin: comparison based on three databases," Fund. Prikl. Gidrofizika **13**, 43—55 (2020). https://doi.org/10.7868/S207366732003003X
9. E. V. Novoselova and T. V.Belonenko, "Isopycnic advection in the Lofoten Basin of the Norwegian Sea," Fund. Prikl. Gidrofizika **13**, 56—67 (2020). https://doi.org/10.7868/S2073667320030041
10. V. S. Travkin and T. V. Belonenko, "Estimation of the winter convection in the Lofoten Basin of the Norwegian Sea and the estimation method," Gidrologiya i Ekologiya (Uch. Zapiski Ross. Gos. Gidrometeorolog. Univ.) **59**, 67—83 (2020). https://doi.org/10.33933/2074-2762-2020-59-67-83
11. A. Fedorov, I. Bashmachnikov, and T. Belonenko, "Winter convection in the Lofoten Basin based on ARGO buoys and hydrodynamic simulation," Vest. St. Petersburg. Univ. Nauki o Zemle **64**, 491—511 (2019). https://doi.org/10.21638/spbu07.2019.308
12. I. Bashmachnikov, T. Belonenko, P. Kuibin, et al., "Pattern of Vertical Velocity in the Lofoten Vortex (the Norwegian Sea)," Ocean Dynamics **68**, 1711—1725 (2018). https://doi.org/10.1007/s10236-018-1213-1

13. T. V. Belonenko, V. S. Travkin, A. V. Koldunov, and D. L. Volkov, "Topographic experiments over dynamical processes in the Norwegian Sea," Russ. J. Earth. Sci. **21**, ES1006 (2021). https://doi.org/10.2205/2020ES000747
14. T. V. Belonenko, V. A. Zinchenko, A. M. Fedorov, et al., "Interaction of the Lofoten Vortex with a satellite cyclone," Pure Appl. Geophysics **178**, 287–300 (2021). https://doi.org/10.1007/s00024-020-02647-1
15. T. Belonenko, V. Zinchenko, S. Gordeeva, and R. P. Raj, "Evaluation of Heat and Salt Transports by Mesoscale Eddies in the Lofoten Basin," Russ. J. Earth Sci. **20**, ES6011 (2020). https://doi.org/10.2205/2020ES000720
16. A. M. Fedorov and T. V. Belonenko, "Interaction of mesoscale vortices in the Lofoten Basin based on the GLORYS database," Russ. J. Earth Sci. **20**, ES2002 (2020). https://doi.org/10.2205/2020ES000694
17. S. Gordeeva, V. Zinchenko, A. Koldunov, et al., "Statistical analysis of long-lived mesoscale eddies in the Lofoten Basin from satellite altimetry," Adv. Space Res. **68** (2020). https://doi.org/10.1016/j.asr.2020.05.043
18. IOC, SCOR and IAPSO. "The international thermodynamic equation of seawater-2010: Calculation and use of thermodynamic properties," in *Intergovernmental Oceanographic Commission, Manuals and Guides*. No. 56, (UNESCO, 2010).
19. R. H. Evens and T. M. Joyce, "Small-scale cyclones on the periphery of Gulf Stream warm-core rings," J. Geophys. Res. **90**, 8845–8857 (1985).
20. S. P. Meacham, K. K. Pankratov, A. F. Shchepetkin, and V. V. Zhmur, "the interaction of ellipsoidal vortices with background shear flows in a stratified fluid," Dynamics of Atmospheres and Oceans **21**, 167–212 (1994). https://doi.org/10.1016/0377-0265(94)90008-6
21. K. K. Pankratov and V. V. Zhmur, "Dynamics of desinglarized quasigeostrophic vortices," Phys. Fluids A **3**, 1464–1464 (1991). https://doi.org/10.1063/1.857998
22. R. P. Raj, I. Halo, S. Chatterjee, et al., "Interaction between mesoscale eddies and the gyre circulation in the Lofoten Basin," J. Geophys. Res.: Oceans **125**, e2020-JC016102 (2020). https://doi.org/10.1029/2020JC016102
23. N. V. Sandalyuk, A. Bosse, and T. V. Belonenko, "The 3D Structure of mesoscale eddies in the Lofoten Basin of the Norwegian Sea: a composite analysis from altimetry and in situ data," J. Geophys. Res.: Oceans **125** (2020). https://doi.org/10.1029/2020JC016331
24. V. S. Travkin and T. V. Belonenko, "Seasonal variability of mesoscale eddies of the Lofoten Basin using satellite and model data," Russ. J. Earth Sci. **19**, ES5004 (2019). https://doi.org/10.2205/2019ES000676
25. D. L. Volkov, T. V. Belonenko, and V. R. Foux, "Puzzling over the dynamics of the Lofoten Basin – a subarctic hot spot of ocean variability," Geophys. Rev. Lett. **40**, 738–743 (2013). https://doi.org/10.1002/grl.50126
26. V. V. Zhmur, E. V. Novoselova, and T. V. Belonenko, "Peculiarities of formation of the density field in mesoscale eddies of the Lofoten Basin: Part 1," Oceanology **61**, 830–838 (2021). https://doi.org/10.1134/S0001437021060333
27. V. A. Zinchenko, S. M. Gordeeva, Yu. V. Sobko, and T. V. Belonenko, "Analysis of mesoscale eddies in the Lofoten Basin based on satellite altimetry," Fund. Prikl. Gidrofzika **12**, 46–54 (2019). https://doi.org/10.7868/S2073667319030067

Translated by I. Melekestseva